Early-Stage Growth of Mn Thin Films Electrodeposited on an Indium Tin Oxide Glass

M. Saitou

Department of Mechanical Systems Engineering, University of the Ryukyus, 1 Senbaru Nishihara-cho Okinawa, 903-0213, Japan
E-mail: saitou@tec.u-ryukyu.ac.jp

Mn thin films grown on indium tin oxide glass in an early-stage electrodeposition were investigated using scanning electron microscopy (SEM) and X-ray diffraction (XRD). SEM images of the Mn thin films showed smooth surfaces comprising steps, terraces, and kinks. Using the SEM images of the steps, we calculated a step fluctuation defined by the standard deviation of the difference between a step and a regression line derived from the step. The step fluctuation was independent of the deposition time and decreased with the deposition temperature. This indicated that the distribution of steps remained in a steady state in an early stage of growth and Mn adatoms moving on the terrace, enhanced by the deposition temperature, suppressed the step fluctuation. XRD analysis revealed that the terrace surfaces were composed of only the (111) planes. The growth of the Mn thin films was consistent with the Frank-van der Merwe mode.

1. INTRODUCTION

Surface dynamics far from thermal equilibrium has attracted scientific interest because understanding the nature of crystalline surfaces at an atomic level is vital for controlling the evolution of the surfaces over time [1–5]. Various microscopic dynamics occur on a vicinal surface comprising steps, kinks, and terraces. Notably, the dynamics of problematic instabilities such as step meandering [6] and step bunching [7] have been a focus of experimental and theoretical research. Steps fluctuate owing to microscopic variations of deposition, surface diffusion, desorption, step attachment or detachment, energy barriers in diffusion fields, and the Ehrlich-Schwöbel (ES) energy barrier [1].

Electrodeposition is a simple and economical method to generate thin films. The surface dynamics of such films require the research of a smooth and vicinal surface observed at an atomic

level. However, in electrodeposition, it has been difficult to obtain a thin film with a smooth surface. This indicates that the growth mode during electrodeposition is not the Frank-van der Merwe (FM) mode, but the Volmer-Weber mode [8]. Electrodeposits grown by the FM mode show surface morphology comprising mounds that obey scaling laws [9]. Hence, the surfaces that evolve with time become roughened. Electrodeposits with atomically smooth surfaces are desirable for the study of the behavior of steps on terraces.

Mn thin films have been reported to be obtained by electrodeposition [10–12]. These studies focused on current efficiencies, which were generally low because of drastic hydrogen evolution during Mn electrodeposition. Scanning electron microscopy (SEM) revealed the surfaces of Mn thin films to have rough surfaces comprising mounds. In this study, we research smooth surfaces of Mn thin films with steps, kinks, and terraces.

The spatial resolution of SEM [13] is in general inferior to scanning tunneling microscopy and atomic force microscopy. A step comprising one atomic monolayer cannot be observed by SEM. However, coarse-grained SEM surface images, which lose information at the atomic scale level, give information of surfaces at a mesoscopic-scale level.

Fluctuation plays an important role in film growth [9]. Time-dependent equations that describe the film growth include a fluctuation term. In this study, a step fluctuation is defined using the standard deviation of the differences in steps. In addition, a regression line derived from the step is introduced to evaluate instabilities in steps.

The aims of the present study are to research Mn thin films comprising steps, kinks, and terraces, the step fluctuation dependent on the deposition temperature, and terraces that have (111) crystallographic planes.

2. EXPERIMENTAL SET UP

An indium tin oxide (ITO) glass of 30×10 mm^2 (the root mean square of the surface roughness was 1.2 nm) and a carbon plate of 35×40 mm^2 were prepared for the cathode and anode electrodes, respectively. An aqueous solution including $MnSO_4 \cdot 5H_2O$ (0.945 mol L^{-1}) and $KNaC_4H_4O_6 \cdot 4H_2O$ (0.65 mol L^{-1}) was prepared. The solution was strained using a membrane with a pore size of 0.1 μm to remove Mn hydroxide particles.

The two electrodes were placed parallel to each other in an electrochemical cell filled with the aqueous solution held within a temperature range of 0–60 °C during electrodeposition. The temperature of the electrochemical cell was controlled using a Peltier controller.

The rectangular pulse voltage was supplied with a function generator. A 22 Ω metal film resistor was connected in series with the electrochemical cell to calculate the current of the rectangular pulse carried between the two electrodes. The rectangular pulse current was used at a frequency of 1 MHz and an amplitude of 4.8 mA cm^{-2} as shown in Fig. 1.

The deposition time in a range of 1–10 s was chosen to investigate surfaces of Mn thin films during early stage electrodeposition. In addition, the deposition time in a range of 100–1000 s was chosen to investigate the crystallographic planes of terraces using X-ray diffraction (XRD).
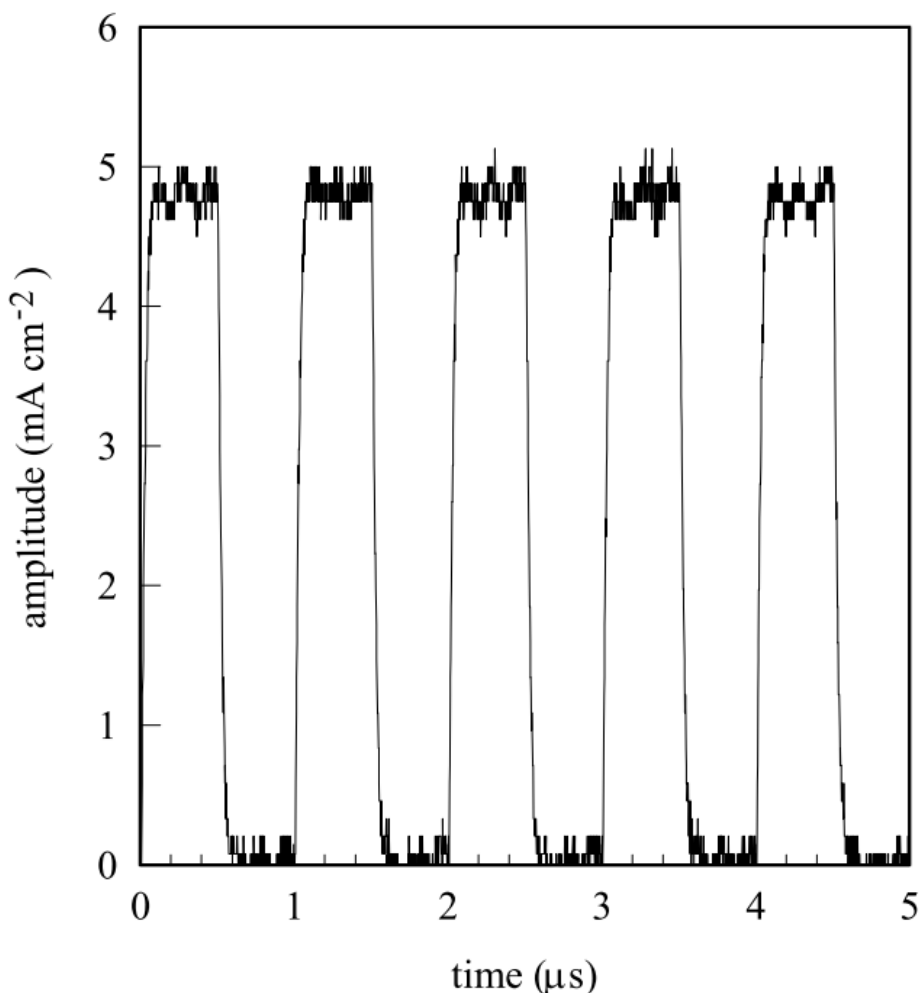
Figure 1. A plot of the rectangular pulse current with an amplitude of 4.8 mA cm^{-2} and a frequency of 1 MHz.

After electrodeposition, Mn thin films generated on the ITO glasses were rinsed with distilled water and put in a vacuum chamber. Their surface morphologies were observed using SEM (Hitachi TM3030). Their crystallographic structures were identified using conventional XRD (Rigaku Ultima) with CuKα radiation and a standard θ-2θ diffractometer with carbon monochromators.

3. RESULTS AND DISCUSSION

All SEM images used in this study have an image size of 640 × 520 pixels. When magnified 30000 times, one pixel in a SEM image corresponds to an area of 8.4 × 8.4 nm^2 on a Mn thin film. As the resolution of SEM is approximately becomes 17 nm, SEM cannot recognize an object less than this resolution. This indicates that the surface images of Mn thin films obtained by our SEM are coarse-grained.
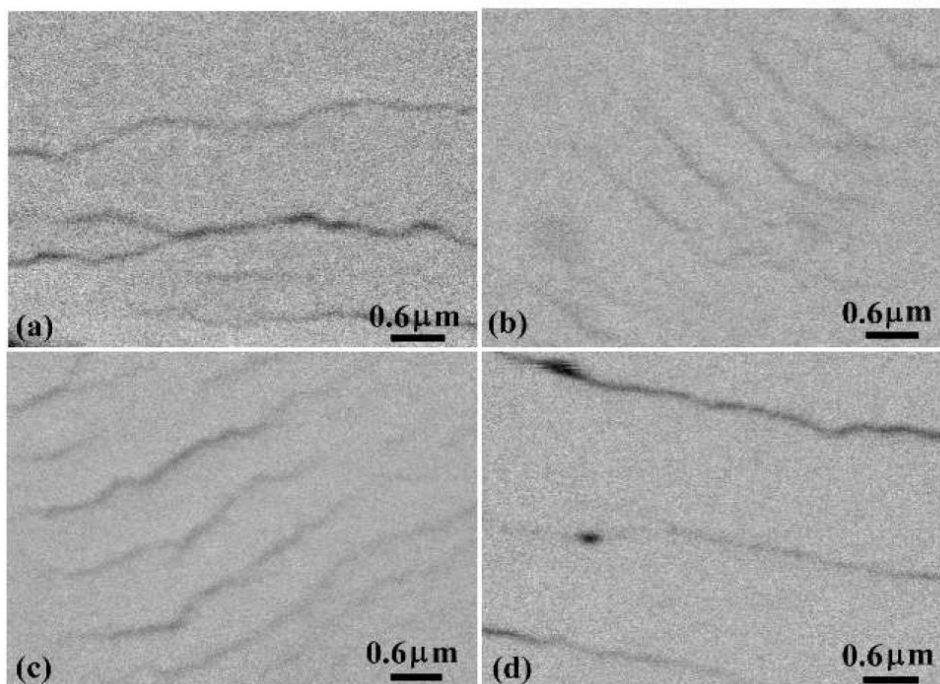
3.1 Mn thin films electrodeposited at 0 ℃

Figure 2. SEM images of Mn thin films electrodeposited at 0 °C for (a) 1, (b) 2, (c) 6, and (d) 10 s.

Typical SEM images of Mn thin films electrodeposited for 1, 2, 6, and 10 s in Fig. 2 show that the film surfaces are composed of steps, kinks and terraces, and are different from surface images of electrodeposits composed of mounds that have been observed in many other studies [9]. The steps in Fig. 2 have a line width larger than the resolution of SEM used in this study. One step on an ideal terrace has a line width approximately equal to the lattice constant, for example, if the terrace of Mn thin film is a (111) plane, the step has a thickness of 0.515 nm. The step with a thickness of the Mn lattice constant cannot be recognized as a line using SEM in this study. Hence, trains of steps and fluctuated steps observed in Fig. 2 indicate that motion of steps causes bunching step. The step bunching allows us to observe the step line as a step using SEM in this study.

In Fig. 2 (b) and (c), trains of steps are located at approximately equal distance despite that the steps meander. In thermal equilibrium, a straight step on an ideal surface is stable [14]. The straight step fluctuates by various kinetic processes such as atoms attaching on the surface, atoms moving on the surface, (which are affected by diffusion potential on a step, kink and terrace), and the ES energy barrier for atom attachment to an ascending and descending step [15–16].

Figure 2 (c) indicates that the steps have similarly fluctuated segments, which are called "in-phase fluctuations". The area in which the steps are in-phase is 3×3 µm^2. In addition, two-dimensional nuclei are not observed on the terraces in Fig. 2. This indicates that all Mn atoms that were generated under a fixed amplitude of the rectangular pulse current moved to steps and kinks.

In non-thermal equilibrium, the estimation of the fluctuation that is time-dependent is very important to understand the film growth [9]. Hence, in this study, the fluctuation step w in two dimensions is defined by

$$w^2 = \frac{1}{L}\int_0^L [\xi(x) - l]^2 dx, \qquad\qquad (1)$$

where L is the step length, $\xi(x)$ is the step, and l is the regression line derived from $\xi(x)$.
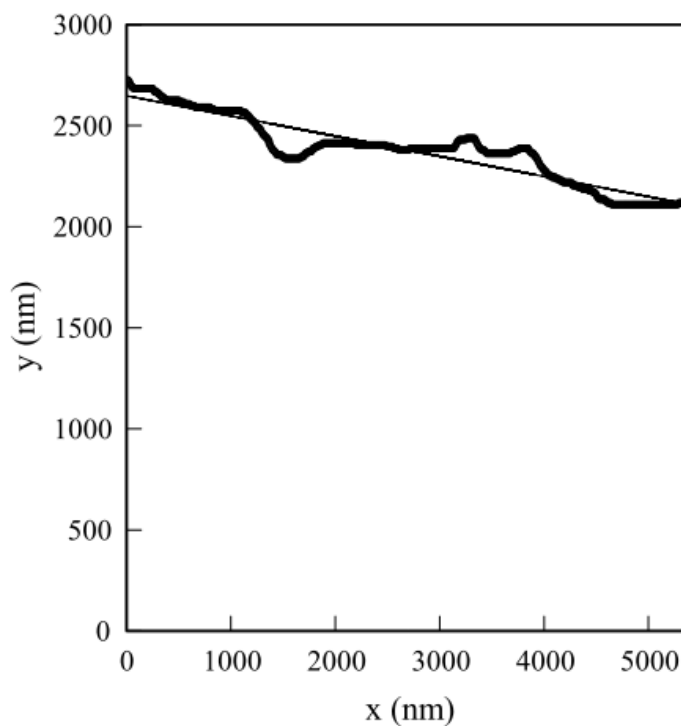

Figure 3. A step extracted from a SEM image of a Mn thin film and a regression line fitted to the extracted step.
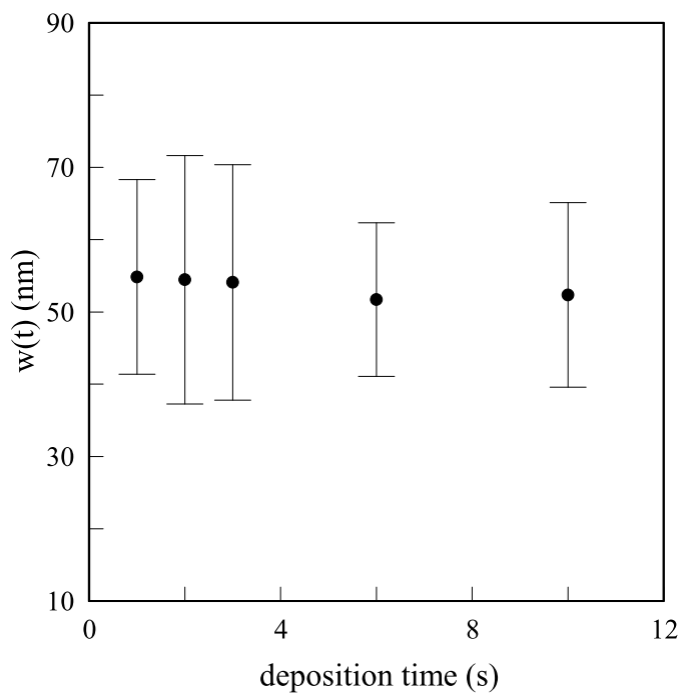

Figure 4. A plot of the fluctuation step w vs. the deposition time using SEM images of Mn thin films electrodeposited at 0 °C.

Figure 3 shows a step extracted from a SEM image of a Mn thin film and a regression line that was processed using the software, "Image J" [17]. The x coordinate axis is taken to be the longitudinal direction of the SEM image.

Figure 4 shows the dependence of the fluctuation step, w, on the deposition time. The fluctuation step is very weakly dependent on the deposition time. The dispersion is due to the meandering of the steps, which yield the large error bar in Fig. 4. Steps, kinks and terraces evolve with the deposition time; however, the distribution of steps does not change with respect to the deposition time.
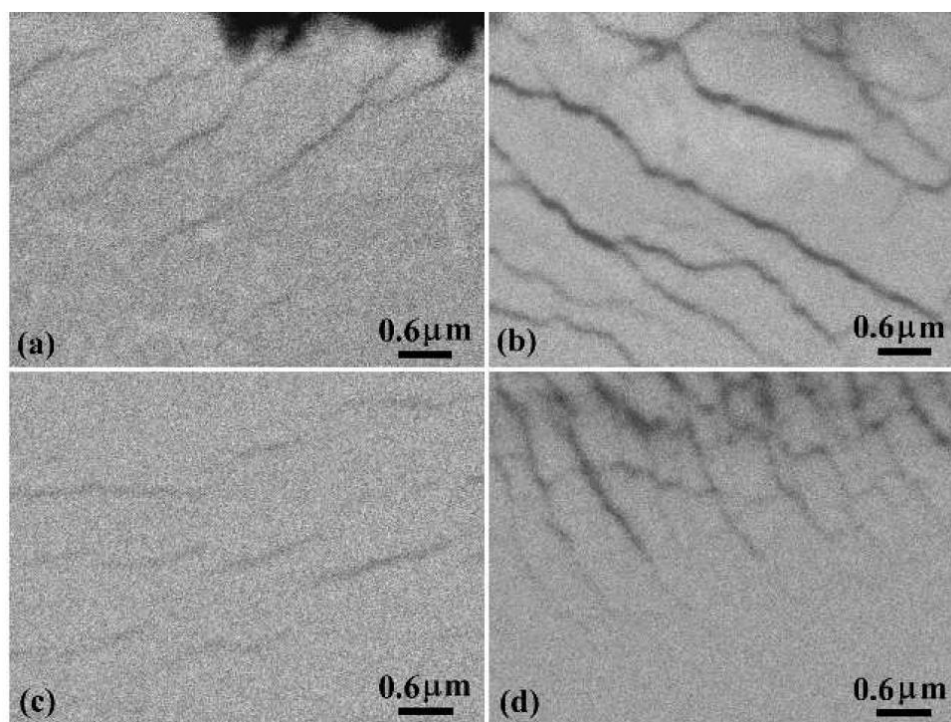
3.2 Mn thin films electrodeposited at 30 ℃

Figure 5. SEM images of Mn thin films electrodepoited at 30 °C for (a) 1, (b) 2, (c) 3, and (d) 6 s.

Figure 5 shows typical SEM images of Mn thin films electrodeposited for 1, 2, 3, and 6 s. In Fig. 5 (a), trains of steps are located at approximately equal distance. In comparison with the steps in Fig. 5 (a), the steps in Fig. 5 (b) meander notably. As there are no nuclei on the terraces, the terraces are denuded zones. In Fig. 5 (c), the steps partially decrease and shorten. Figure 5 (c) is thought to show the process of the step decrease. In the same way, the edges of the steps decrease in Fig. 5 (d).

Figure 6 shows the dependence of the fluctuation step, w, on the deposition time. The fluctuation step is very weakly dependent on the deposition time similar to the fluctuation step in Fig. 4. Hence, the distribution of steps does not change with respect to the deposition time. The mean fluctuation step w is smaller than that at 0 °C.
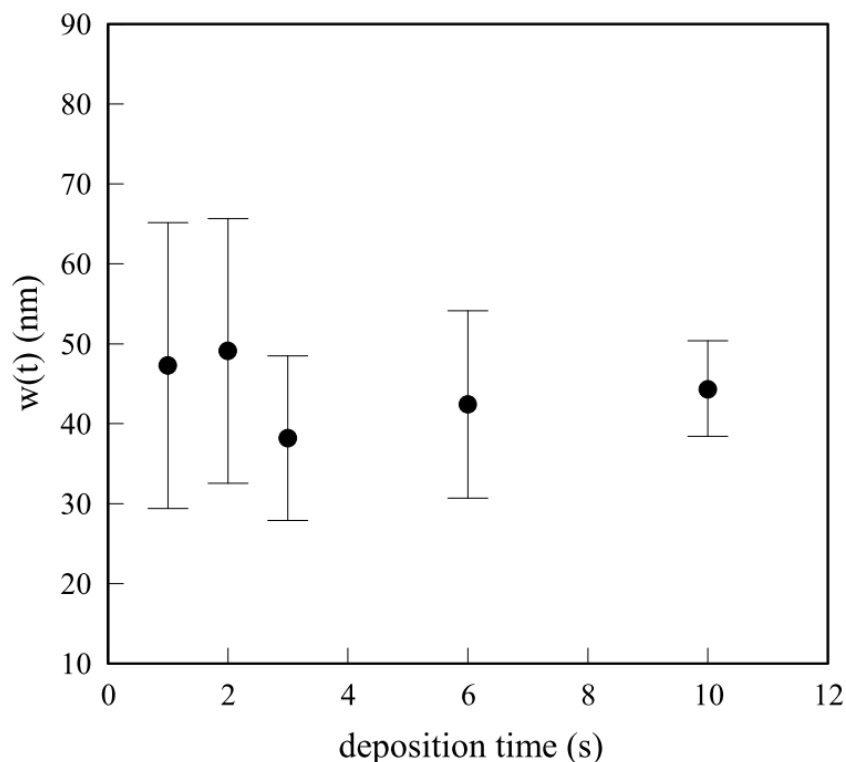
Figure 6. A plot of the fluctuation step w vs. the deposition time using SEM images of Mn thin films electrodeposited at 30 °C.

3.3 Mn thin films electrodeposited at 60 °C

Figure 7 shows typical SEM images of Mn thin films electrodeposited for 1, 2, 3, and 10 s. Trains of steps located at approximately equal distance are not observed. In comparison with steps in Mn thin films electrodeposited at 0 °C, the steps with a short length are dominant. In theories of meandering steps [1, 4], the terrace width defined by the distance between neighboring steps increases with temperature. This indicates that steps with short distances decrease with an increase in temperature. An increase in the deposition temperature enables Mn adatoms to jump the diffusion barrier potential and ES barrier potential. Hence, steps with short distances are likely to decrease owing to Mn atoms moving around on the narrow terrace. The step fluctuation will also decrease with the deposition temperature.

Figure 8 shows the dependence of the fluctuation step, *w*, on the deposition time. The fluctuation step is very weakly dependent of the deposition time similar to the fluctuation step at 0 and 30 °C. In comparison with the fluctuation step of the Mn thin films electrodeposited at 0 °C, the fluctuation step in Fig. 8 is smaller. This means that a greater number of Mn atoms allow steps to move forward under a fixed amplitude of the rectangular pulse current. Hence, the terrace width will increase with the deposition temperature as well as the theoretical derivation [1].
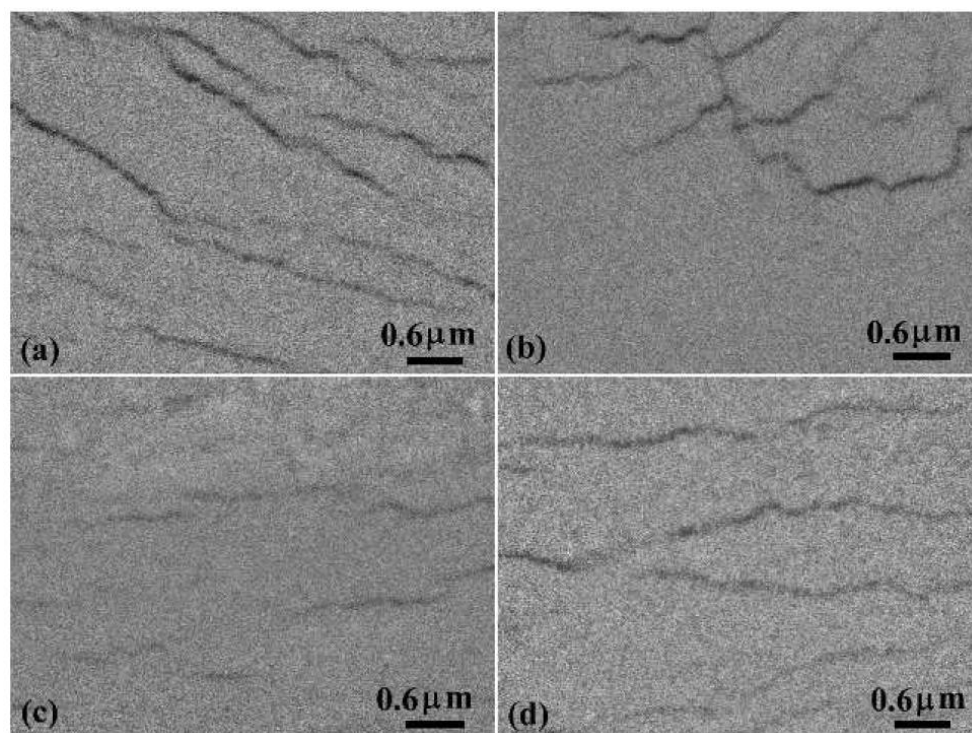
Figure 7. SEM images of Mn thin films electrodepoited at 60 °C for (a) 1, (b) 2, (c) 3, and (d) 10 s.
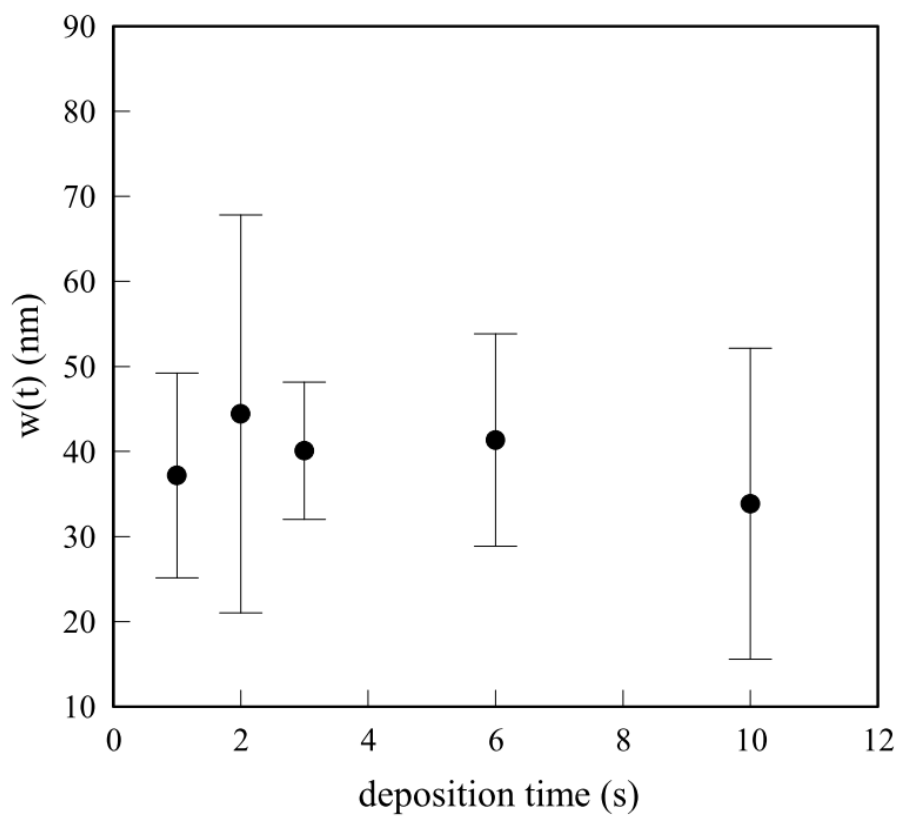

Figure 8. A plot of the fluctuation step *w* vs. the deposition time using SEM images of Mn thin films electrodeposited at 60 °C.
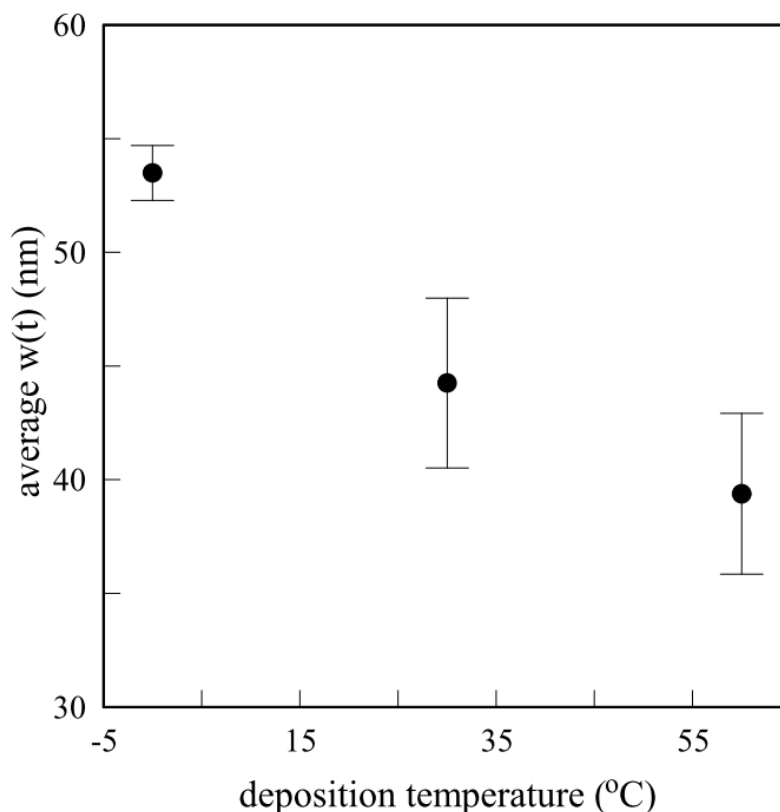
Figure 9. A plot of the average fluctuation step *w* vs. the deposition temperature.

Taking the average of the fluctuation step *w* on the deposition time range of 1–10 s in Figs. 4, 6, and 8, we obtain a plot of the average *w* vs. the deposition temperature as shown in Fig. 9. Figure 9 shows the dependence of the average fluctuation step, *w*, on the deposition temperature. The fluctuation step decreases with the deposition temperature. This is likely due to Mn adatoms, which, at a higher temperature, can move a longer distance on a terrace. Hence, the Mn adatoms do not accelerate, but suppress the fluctuation of steps.

3.4 Crystallographic planes of terraces determined by XRD

Figures 10 (a), (b), and (c) show XRD patterns of Mn thin films electrodeposited for 100, 300, and 1000 s, respectively. All the diffraction peaks indexed as the (222) planes [18] are consistent with those of α-Mn. This indicates that the surfaces of the terraces shown in Figs. 2, 5, and 7 are the (111) planes, which are parallel to the ITO glass. The crystal structure of α-Mn is a complex structure with 58 atoms in the cubic cell [19], which is similar to the body-centered cubic structure (BCC). In iron electrodeposition (α-Fe: BCC), a thin film that has only one crystallographic plane parallel to a substrate was reported to be grown [20]. The iron thin film surface appeared to be mirror like. Similarly, the surfaces of Mn thin films electrodeposited for 10–1000 s were also smooth.
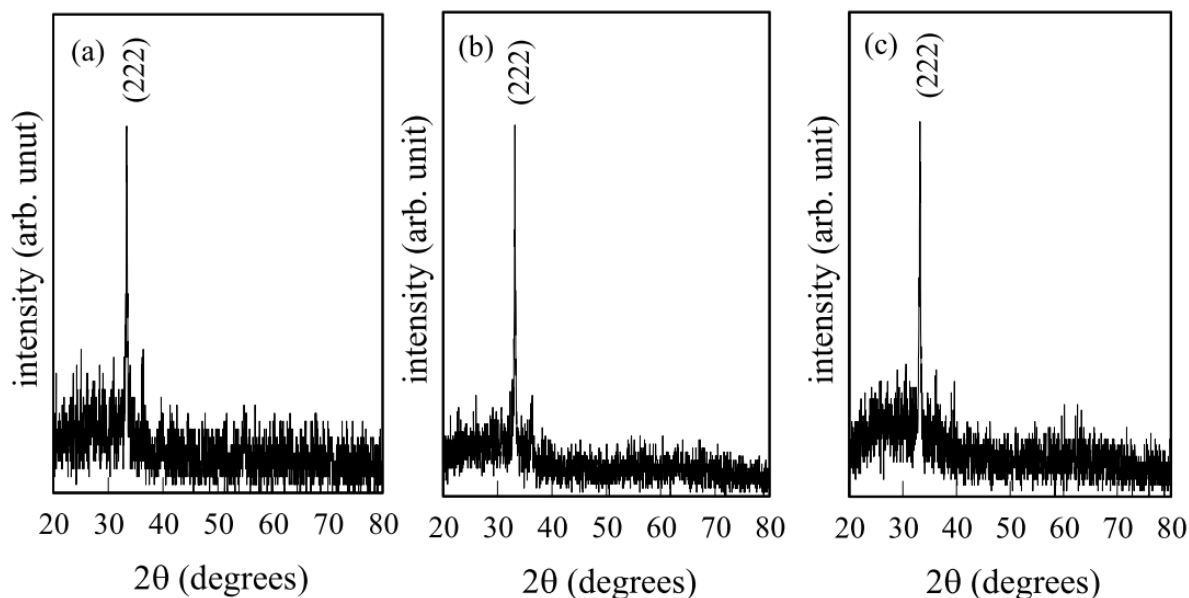
Figure 10. XRD patterns of Mn thin films electrodeposited at 60 °C for (a) 100, (b) 300, and (c) 1000 s. All the Mn thin films were electrodeposited at an amplitude of 4.8 mA cm^{-2} and 1 MHz.

Steps that move on the (111) plane result in step bunching. The Mn film growth is the layer by layer growth, i.e., the FM mode [8].

4. CONCLUSIONS

In this study, we investigated the Mn thin films grown on indium tin oxide glasses in early stage electrodeposition. The SEM images of the Mn thin films were the smooth surfaces comprising steps, terraces, and kinks. The step fluctuation was found to be independent of the deposition time but decrease with the deposition temperature. This indicated that the distribution of steps was in a steady state and Mn adatoms moving on the terrace suppressed the step fluctuation. XRD analysis revealed that the surfaces of Mn thin films were composed of only the (111) planes. The growth of the Mn thin films was consistent with the FM mode.

References

1. C. Misbah, O. P-Louis and Y. Saito, *Rev. Mod. Phys.*, 82 (2010) 981.
2. D.I. Rogilo, L.I. Fedina, S.S. Kosolobov, B.S. Ranguelov and A.V. Latyshev, *Phys. Rev. Lett.*, 111 (2013) 036105.
3. T.L. Einstein, *Appl. Phys. A*, 87 (2007) 375.
4. H-C Jeong and E.D. Williams, *Surf. Sci. Rep.*, 34 (1999) 171.
5. L. Persichetti, A. Sgarlata, M. Fanfoni and A. Balzarotti, *J. Phys. Condens. Matter.*, 27 (2015) 253001.
6. X.–S. Wang, J.L. Goldberg, N.C. Bartelt, T.L. Einstein and E.D. Williams, *Phys. Rev. Lett.*, 65 (1990) 2430.
7. A.V. Latyshev, L.V. Litvin and A.L. Aseev, *Appl. Surf. Sci.*, 130-132 (1998) 139.

8. G.F. Gilmer, M.H. Grabow and A.F. Bakker, *Mater. Sci. Eng.*, B6 (1990) 101.
9. A.-L. Barabási and H.E. Stanley, *Fractal Concepts in Surface Growth*, Cambridge, Cambridge Uni. Pr., 1995.
10. J-K. Chang, W-T. Tsai, P-Y. Chen, C-H. Huang, F-H. Yeh and I-W. Sun, *Electrochem. Solid-State Lett.,* 10 (2007) A9.
11. S.K. Padhy, P. Patnaik, B.C. Tripathy, M.K. Ghosh and I.N. Bhattachary, *Hydrometallurgy,* 165 (2016) 73.
12. J. Lu, D. Dreisinger, and T. Glück, *Hydrometallurgy*, 141 (2014) 105.
13. J.R. Michael, *Scanning*, 22 (2011) 147.
14. W.K. Burton, N.Cabrera and F.C. Frank, *Proc. R. Soc. Lond. A,* 243 (1951) 299.
15. G. Ehrlich and F. Hudda, *J. Chem. Phys.*, 44 (1966) 1039.
16. R. Schwoebel and E. Shipsey, *J. Appl. Phys.*, 37 (1966) 3682.
17. https://imagej.nih.gov/ij/
18. J.A. Oberteuffer and J.A. Ibers, *Acta Cryst.*, B26 (1970) 1499.
19. D. Hobbs, J. Hafner and D. Spišák, *Phy. Rev. B*, 68 (2003) 014407.
20. M. Saitou, *Int. J. Electrochem. Sci.*, 12 (2017) 1885.